Sensor and Simulation Notes
Note 292
1 May 1986

DESIGN PROCEDURES FOR ARRAYS WHICH APPROXIMATE A DISTRIBUTED SOURCE AT THE AIR-EARTH INTERFACE

Y.-G. Chen, S. Lloyd and R. Crumley
Maxwell Laboratories, Inc., San Diego, CA

Carl E. Baum
Air Force Weapons Laboratory

and

D.V. Giri
Pro-Tech, 125 University Avenue, Berkeley, CA 94710

Abstract

This note addresses a general electromagnetic problem of simulating a distributed source at an interface of a conducting dielectric by an array of pulsers. One possible application lies in the simulation of the distributed source at the air-earth interface associated with a nuclear EMP [1]. Other electromagnetic applications may include geological prospecting, detection of buried objects and study of the coupling of the field generated by natural lightning to underground objects. In general, the design procedures of arrays approximating distributed sources considered here are applicable whenever, a need for coupling electromagnetic waves into earth arises. Approximate theoretical considerations, as well as design procedures for the arrays are discussed.

WL-EMP-SSN-293
Sensor and Simulation Notes
Note 292
1 May 1986

DESIGN PROCEDURES FOR ARRAYS WHICH APPROXIMATE A DISTRIBUTED SOURCE AT THE AIR-EARTH INTERFACE

Y.-G. Chen, S. Lloyd and R. Crumley
Maxwell Laboratories, Inc., San Diego, CA

Carl E. Baum
Air Force Weapons Laboratory

and

D.V. Giri
Pro-Tech, 125 University Avenue, Berkeley, CA 94710

Abstract

This note addresses a general electromagnetic problem of simulating a distributed source at an interface of a conducting dielectric by an array of pulsers. One possible application lies in the simulation of the distributed source at the air-earth interface associated with a nuclear EMP [1]. Other electromagnetic applications may include geological prospecting, detection of buried objects and study of the coupling of the field generated by natural lightning to underground objects. In general, the design procedures of arrays approximating distributed sources considered here are applicable whenever, a need for coupling electromagnetic waves into earth arises. Approximate theoretical considerations, as well as design procedures for the arrays are discussed.

Keywords: dielectrics, pulser array, effects of nuclear blast

FOREWORD

The authors are thankful to Mr. W. Walton, Mr. D. Craig and Lt. J. Crissey of the Air Force Weapons Laboratory who have provided encouragement and support at various stages of this effort. Thanks are also due to Mr. B. Barton and Mr. P. Elliott of Maxwell Laboratories, Inc. for their assistance.

CONTENTS

I. Introduction

A general electromagnetic problem of simulating a distributed source near an interface of a conducting dielectric is addressed in this note. There exist many possible applications for such a source. These include simulation of the distributed source near an interface caused by a nuclear EMP, considered in some detail in [1]. Geological prospecting and detection of buried objects such as underground tunnels are also among possible applications. The need in practice is to simulate the large distributed source by a suitable collection of 'point' sources. We are concerned here with some aspects of realization of a distributed source with discrete sources.

We consider a general technique of arraying pulse generators at an air-earth interface with the view of producing certain electromagnetic environment in the lossy medium. Certain aspects of such distributed sources were considered in earlier works [2 to 5]. For the present, our interest is in simulating the distributed source by transient pulse generators and associated design considerations, including ways of launching the wave from the pulser output switch onto the interface.

In this technique, the discrete sources are placed at the interface and there could be a relatively highly conducting, non-magnetic medium between the distributed source and earth's surface. If such a medium is employed, it should be relatively thin to allow the high frequencies from the distributed source to propagate through it to some portions of the system to be exposed near the interface. The distributed source is intended to be placed over those portions of the underground site, which are near or even protrude above the earth's surface.

Another important aspect of such a technique is that the fast rising pulsers in the distributed source are triggered sequentially across the site to yield a propagation speed (phase velocity) greater than or equal to that of the speed of light c in air. Furthermore, the amplitudes of the pulse generators can be decreasing in the direction of propagation, if the intended application requires such a decaying amplitude.

In this note attention is focussed on approximation of the distributed source by a two dimensional array of pulsers. Section II describes the requirements of the distributed source while Section III considers the distributed source as an array. The practical considerations in going from the output switch in an individual pulse generator to an electromagnetic wave incident on the interface form the subject of Section IV. The note ends with a summarizing Section V followed by a list of references.

II. Distributed Source

The underlying idea of the present technique is to approximately generate some important features of the electromagnetic fields required to be produced underground, by a two-dimensional array of pulse sources near the interface. The basic geometry is shown in figure 2.1, indicating a distributed source at a height h above the interface between the two media. Ground is the lower medium ($z < 0$) with constitutive parameters ε_2, μ_o and σ_2. The region extending from $0 < z < h$ could be air or a thin conducting medium represented by parameters ε_1, μ_o and σ_1, depending on the intended application and the level of sophistication in producing the required underground fields. All parameters are assumed to be independent of the y coordinate and furthermore, the finite extents in $+x$ and $-x$ directions are also ignored. Note that if medium 1 is unionized air, we may approximate $\varepsilon_1 \simeq \varepsilon_o$ and $\sigma_1 = 0$.

The characteristic feature of the distributed source is such that it establishes a tangential electric field (i.e., x directed) on its plane at $z = +h$, of the time-domain form [5],

$$E_s(x,y,h,t) = E_o(t - \frac{x}{v})\, e^{-x/\chi} \qquad (2.1)$$

where

E_o = transient waveshape, which is constant in retarded time

v = speed of light in medium 1 $\equiv (\mu_o \varepsilon_1)^{-\frac{1}{2}}$.

The above source field also exhibits an exponential attenuation along the x direction with an e-folding distance of χ that could correspond to a decreasing amplitude in the direction

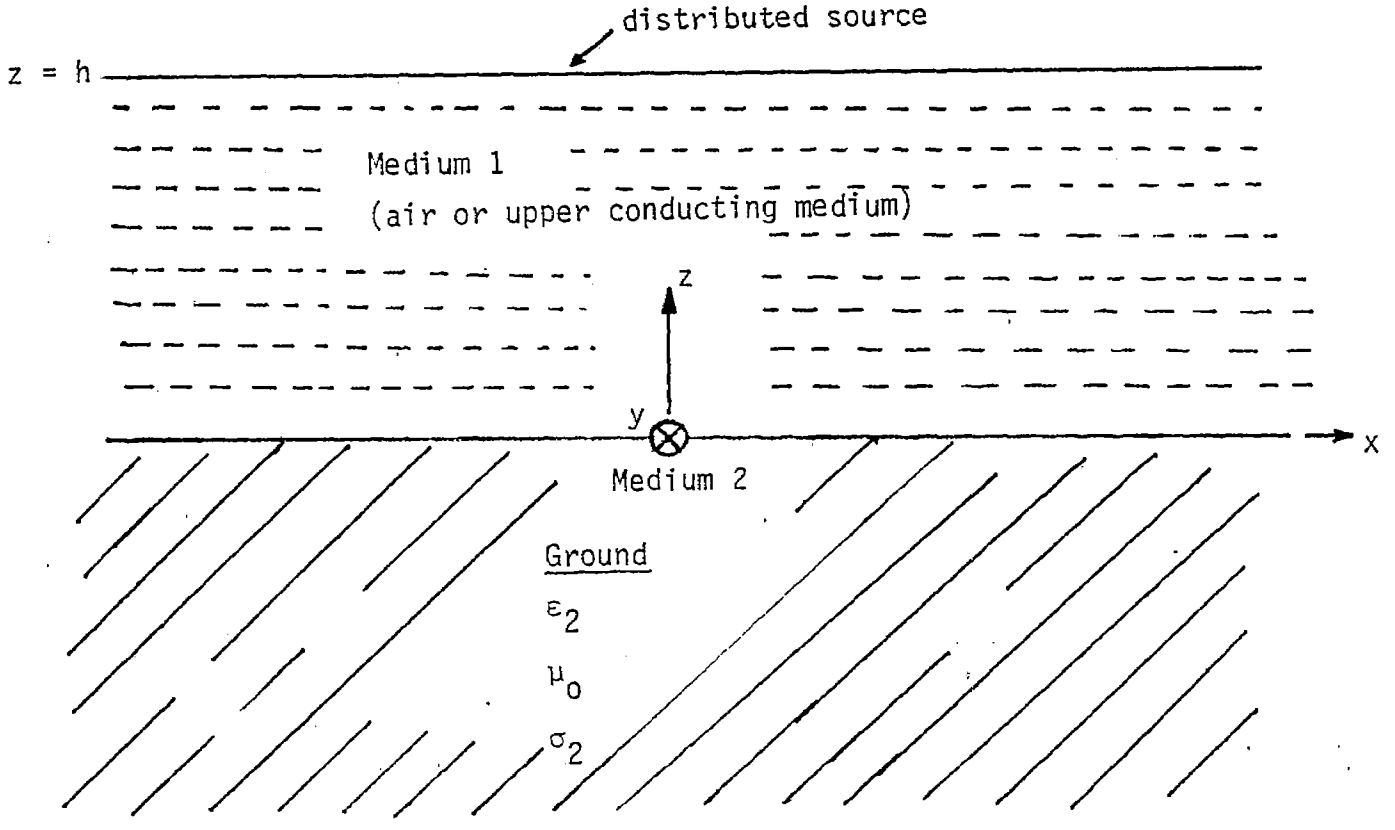

Figure 2.1. Distributed source near the interface.

of wave propagation. In the frequency domain, if the familiar two-sided Laplace transformation to complex frequency $s \equiv (\Omega + j\omega)$ is used, (2.1) becomes

$$\tilde{E}_s(x,y,h,s) = \tilde{E}_o(s)\, e^{-\gamma_s x} \tag{2.2}$$

with

$$\gamma_s = \gamma + \frac{1}{\chi} = (\frac{s}{v} + \frac{1}{\chi}) \tag{2.3}$$

It is noted that the exponential attenuation in the x direction in (2.1), conveniently becomes a part of the propagation constant γ_s in the frequency domain source equation above.

If the intended application is attempting to simulate close-in EMP for instance, the source field described above is similar to an EMP source near an air-earth interface in many important respects as noted below:

a) it propagates at a speed $\geq c$

b) its amplitude attenuates in a manner consistent with that of the source

c) resulting fields and current densities can approximate the same x-dependence as the source field.

It is also emphasized however, that typically σ_1 and ε_1 are taken as constants independent of time and position, which is not in general the case in the nuclear EMP environment.

Observe that the source field prescribed above is the tangential electric field and could well have been the tangential magnetic field. The uniqueness of solutions of Maxwell's equations [6,7] is preserved under either prescription of the source field.

In proving the uniqueness, one assumes two possible solutions with the same given tangential field on the boundary of the region of interest. The difference field is formed and found to satisfy a Poynting's theorem. Stratton [6] then shows that for linear, isotropic (but possibly inhomogeneous) media, specification of tangential $\vec{E}$ and $\vec{H}$ on the boundary and the initial values at time zero, is sufficient to specify fields uniquely within the region at all times $t > 0$. The argument can be extended to anisotropic materials and certain classes of nonlinear materials but not to materials that have multivalued relationships between $\vec{D}$ and $\vec{E}$ (or $\vec{B}$ and $\vec{H}$). Although the uniqueness discussion is in the context of regions with closed boundaries, it also applies to open regions extending to infinity (or "closed at infinity"), provided certain radiation conditions are satisfied by the fields. It is required that the products of $r\vec{E}$ and $r\vec{H}$ remain finite as r approaches infinity. In our present concept of a distributed source, the source field is specified on a boundary ($z = h$) that extends to infinity. Furthermore, the fields arising from true charge and current sources contained within a finite region in practice, do satisfy the radiation conditions. The specification of the tangential electric source field as opposed to the tangential magnetic field [2] has practical significance since, from an engineering point of view, the electric source field can be realized by an array of slats excited by a set of pulsers triggered in an appropriate sequence. In other words, practical considerations require that the 'theoretically' convenient distributed source be replaced by a collection of discrete sources. Such a practical approximation of the distributed source by an array of discrete pulsers is the subject of the following section.

III. Distributed Source As an Array

The desired form of the electromagnetic wave discussed in the previous section applies directly to the high-frequency or early-time part of the distributed source located physically above that part of the system under exposure which are near the surface. It is only these portions of the system that are 'driven' by the localized high-frequency sources. Practical sources, e.g., charged capacitors and switches are discrete and hence the distributed sheet source can only be realized by an array of pulser modules. This matrix of modules is interconnected, charged and triggered in a way that approximates the desired sheet source.

Having said that we have an array of high frequency or early-time modules, to be distributed in two dimensions (x and y directions) at $z = +h$, two design choices are considered. They are i) in-line configuration and ii) staggered configuration discussed below.

A. In-line configuration

This configuration is illustrated in figure 3.1 (reproduced from [4]) with a 3×3 array of 9 modules and covering approximately a rectangular area of the upper medium 1. P, Q, R and S form a unit cell in this arrangement with $PQ = RS = \Delta x$ and $QS = PR = \Delta y$ being the spacing along the x and y directions respectively. Such an arrangement is simple and results from an attempt to minimize the maximum time from a pulser module to any point on the interface. For the present, if all the modules are switched on simultaneously, the above criterion leads to a square unit cell where in $\Delta x_o = \Delta y_o$, corresponding to a maximum transit distance of

$$\sqrt{(\Delta x_o/2)^2 + (\Delta y_o/2)^2} = \Delta x_o/\sqrt{2} = \Delta y_o/\sqrt{2}$$

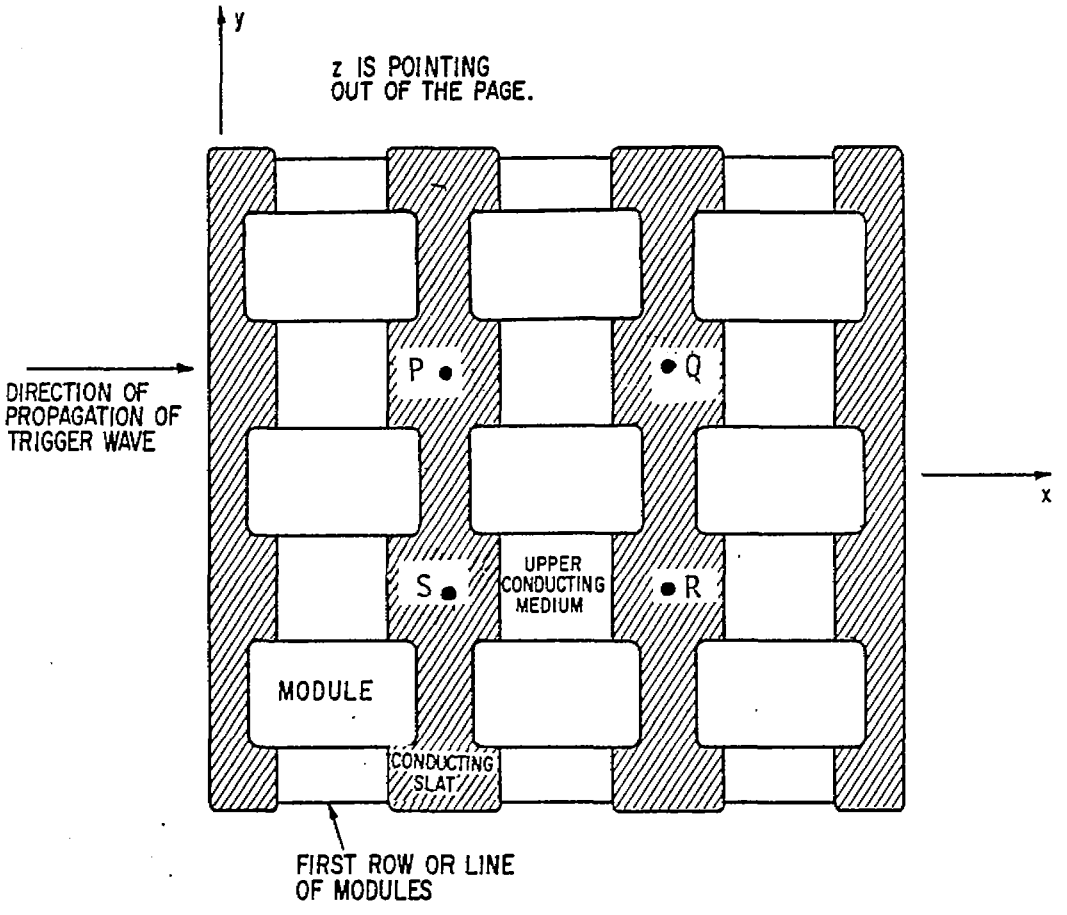

(a) Top View

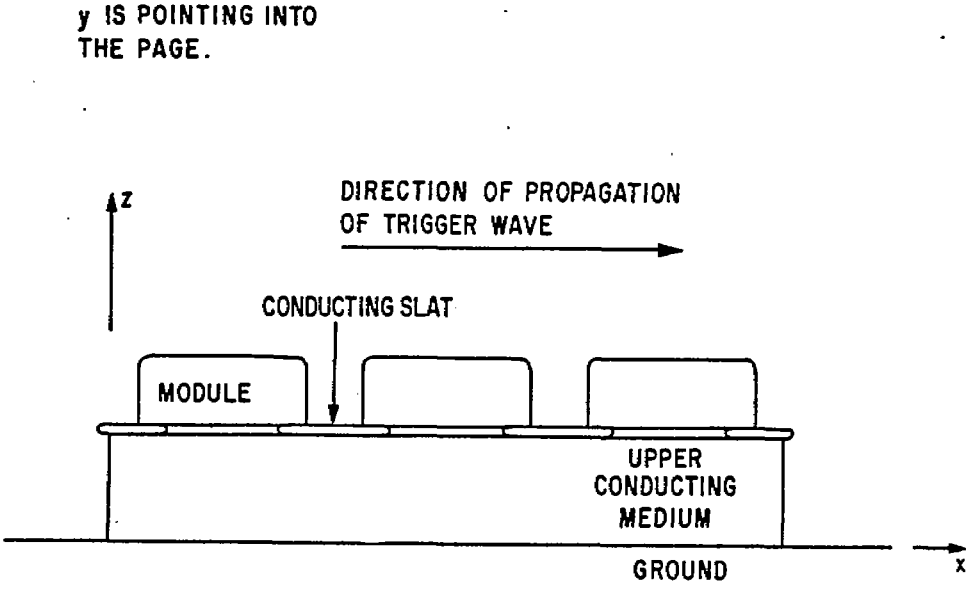

(b) Side View

Figure 3.1. High frequency modules arranged in an in-line configuration [4].

A 3 x 3 array of modules is considered only for illustrative purposes and typically a much larger number of modules is desirable for improved uniformity and rise characteristics of the electromagnetic wave. The general lay-out consists of conducting slats along the y-direction i.e., perpendicular to the desired electric field direction. These slats not only interconnect the modules but also provide electrical contact with the medium occupying the region $0 < z < h$. Between two adjacent conducting slats is a row of modules, which are simultaneously triggered establishing a potential drop and consequently an x-directed electric field between adjacent slats. Successive rows are triggered sequentially in the order of increasing x at times that simulate a wave propagating in the $+x$ direction at speed greater than or equal to that of light c in free space. Within each row, the triggered signal is distributed by electrical cables.

In order to improve the high frequency performance, an alternative staggered configuration is feasible as described below.

B. Staggered configuration

Consider a staggered arrangement of the modules as indicated in figure 3.2 with spacings of Δx and Δy along the x and y directions respectively. The criterion of minimizing the maximum transit time to any point on the array, under the assumption of simultaneous firing of <u>all</u> modules, leads to an interesting result. By choosing for example $(\Delta x/\Delta y) = 0.5$ and neglecting the height h of the distributed source, the maximum transit distance for a given unit cell area is $\Delta x = \Delta y/2$ which is an improvement over $\Delta y/\sqrt{5/16}$ if the modules were in an in-line arrangement, under the same assumption of $\Delta x = \Delta y/2$.

The above outlined staggered configuration appears to be more efficient if one were interested in a large two dimensional array of modules. It is noted that the spacing along the direction of the electric field (x direction) if one half the spacing along the direction perpendicular to the electric field (y direction).

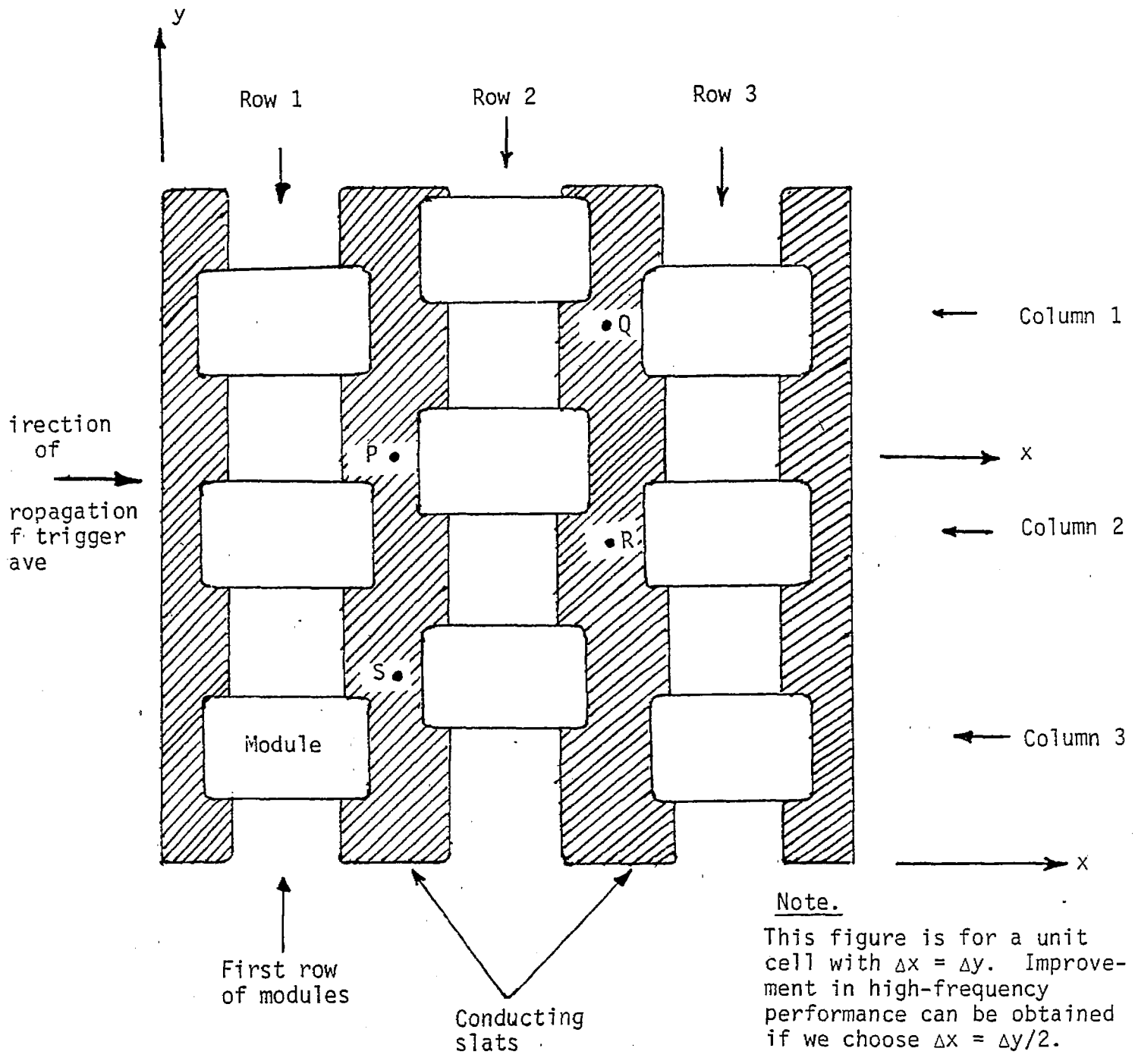

Figure 3.2. Top view of high frequency modules arranged in a staggered configuration.

In concluding this section, we may note a convention in representing the various modules. Specifically, a matrix numbering scheme is useful for the modules. The rows are along the y direction and the columns are along the x or electric field direction. So an (i, j) th module would then be located in the i th row and j th column. One could also choose the lower left corner of the array in its top view as the origin of a rectangular coordinate system (x, y, z) for convenience.

Next, we turn our attention to the design considerations in going from the 'switch gap' in the module to earth in a unit cell, in the following section.

IV. Design Considerations for Getting from Switch to Earth in Unit Cell

There are many electromagnetic as well as practical design considerations in going from the switch gap in the module to the air-earth interface. The problem here is one of placing suitable electrical conductors from the pulser modules to and including the ground contacts or slats. The electromagnetic considerations underlying this problem are discussed in this section under three separate headings.

A. Brewster Angle Wave Launcher

A technique, utilizing the concept of a high-frequency Brewster angle has been analyzed in the past [8], for placing fast-rising transient electromagnetic fields over a ground surface.

Consider the problem of "matching" a pulsed wave into ground, when the assumed incident plane wave is polarized such that its magnetic field is parallel to the ground surface, as illustrated in figure 4.1. For such a polarization, and for frequencies much greater than the relaxation frequency (σ/ε) of the ground medium, there is an angle of the incident wave at which there is insignificant reflection of the incident wave from the ground surface. This angle is termed the high-frequency Brewster angle [8].

With reference to figure 4.1, the reflection coefficient in frequency domain for a step-function pulse is given by [8],

$$\tilde{R}_h(s) = \frac{1}{s_r} \frac{\cos(\theta_1) - \sqrt{\frac{1}{\varepsilon_r} \frac{s_r}{1+s_r} \left[1 - \frac{1}{\varepsilon_r} \frac{s_r}{1+s_r} (\sin(\theta_1))^2\right]}}{\cos(\theta_1) + \sqrt{\frac{1}{\varepsilon_r} \frac{s_r}{1+s_r} \left[1 - \frac{1}{\varepsilon_r} \frac{s_r}{1+s_r} (\sin(\theta_1))^2\right]}} \qquad (4.1)$$

where

$\sim$ over a quantity indicates Laplace transformed quantity

$s_r \equiv$ normalized complex frequency $= st_r = st/t_r$

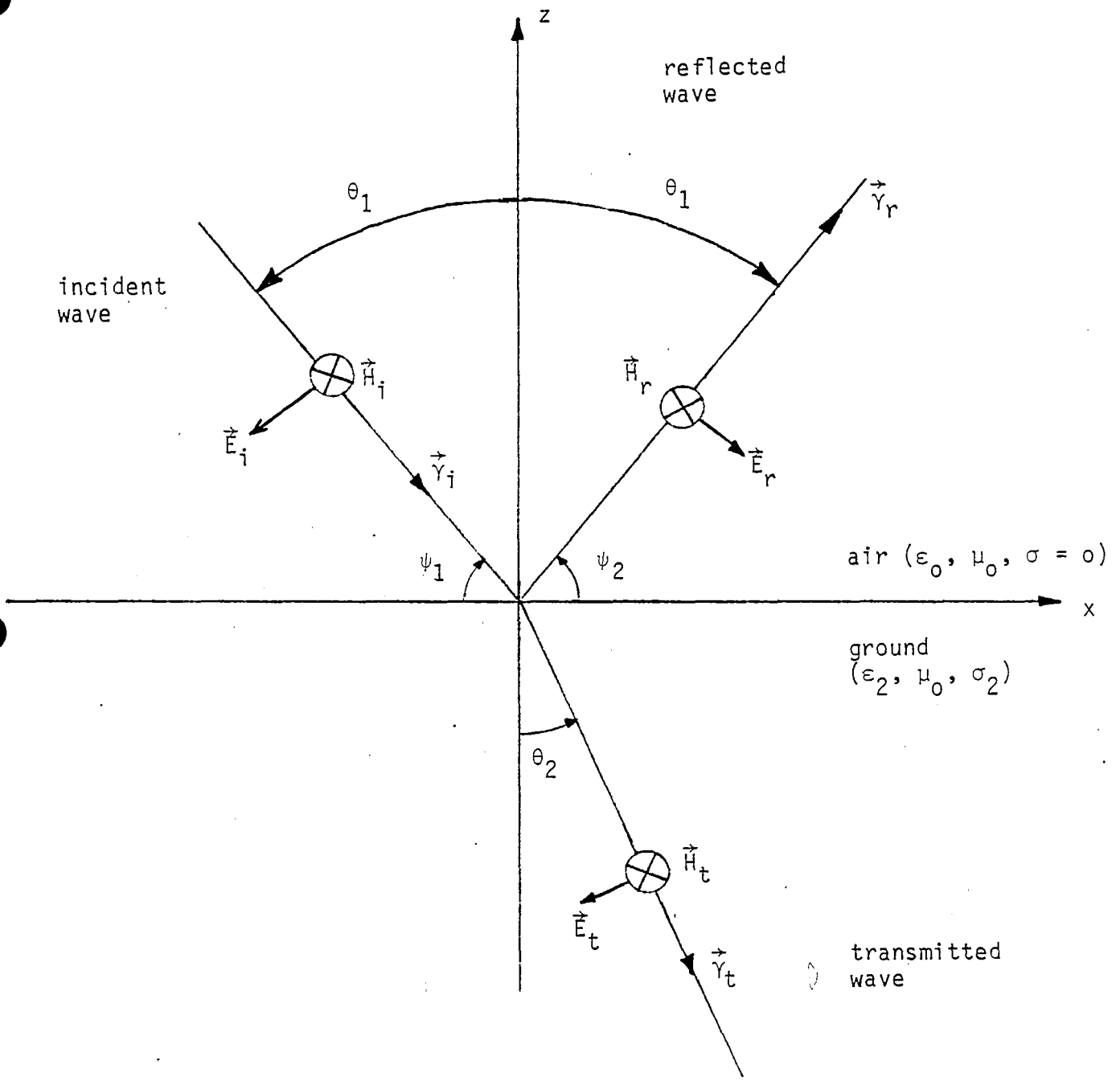

Figure 4.1. Incident plane wave with its magnetic field parallel to the interface between air and ground media.

$s \equiv$ complex frequency

$t \equiv$ time variable

$t_r \equiv$ normalized time $= \varepsilon_2/\sigma_2 = \varepsilon_r\varepsilon_0/\sigma_2$ (4.2)

$\theta_1 \equiv$ incident angle

In time domain, the initial rise of R_h is given by [9]

$$R_h(t = 0^+) = \lim_{s \to \infty} \left\{ s\tilde{R}_h(s) \right\}$$

$$= \left[\frac{\cos(\theta_1) - \frac{1}{\varepsilon_r}\sqrt{\varepsilon_r - (\sin(\theta_1))^2}}{\cos(\theta_1) + \frac{1}{\varepsilon_r}\sqrt{\varepsilon_r - (\sin(\theta_1))^2}} \right] \tag{4.3}$$

Setting the above quantity to zero defines the high-frequency Brewster angle as

$$\cos(\theta_B) = \frac{1}{\sqrt{1 + \varepsilon_r}} \tag{4.4}$$

or

$$\sin(\theta_B) = \sqrt{\frac{\varepsilon_r}{1 + \varepsilon_r}} \tag{4.5}$$

There is also a more convenient relationship

$$\tan(\psi_B) = \cot(\theta_B) = 1/\sqrt{\varepsilon_r} \tag{4.6}$$

recalling that angles ψ and θ are measured from the interface and its normal respectively. Although, ε_r of soil is frequency dependent, it appears to level off at high frequencies [10]. An example value of $\varepsilon_r = 10$ results in $\psi_B \simeq 17.6°$.

As was pointed out earlier, this high-frequency Brewster angle concept is valid for times of the order of relaxation time of the ground. The ground medium behaves like a conductor at low frequencies and like a dielectric at high frequencies. Equivalently, it starts out as a dielectric at early times and then transitions into a conductor at later times and the relaxation time is some measure of the characteristic time t_r which the Brewster angle concept is valid. Such a characteristic time t_r was used earlier in normalizing the frequency variable, and is given by

$$t_r = (\varepsilon_2/\sigma_2) = (\varepsilon_o\varepsilon_r/\sigma_2) \tag{4.7}$$

In this time, an electromagnetic wave in air (above the ground) propagates a distance

$$d_r \equiv ct_r = \frac{c\,\varepsilon_o\varepsilon_r}{\sigma_2} = \frac{\varepsilon_r}{Z_o\sigma_2} \tag{4.8}$$

with

$$Z_o \equiv \sqrt{\frac{\mu_o}{\varepsilon_o}} \quad \text{(free space wave impedance)}$$

$$\simeq 377\ \Omega \tag{4.9}$$

Consider some typical values as indicated below.

$$\begin{aligned}
&\text{example i)} \quad \varepsilon_r = 10 \quad , \quad \sigma_2 = 10^{-2} \text{ S/m} \\
&\qquad\qquad t_r \simeq 8.85 \text{ ns} \quad , \quad d_r \simeq 2.65 \text{ m} \\
&\text{example ii)} \quad \varepsilon_r = 10 \quad , \quad \sigma_2 = 10^{-3} \text{ S/m} \\
&\qquad\qquad t_r \simeq 88.5 \text{ ns} \quad , \quad d_r \simeq 26.5 \text{ m}
\end{aligned} \tag{4.10}$$

The above examples indicate that for unit cell dimensions of the order of 1 m the high-frequency Brewster angle concept is approximately valid.

In order to minimize early time reflections using the above outlined Brewster-angle concept, one may consider a unit cell geometry illustrated in figure 4.2. Both top and side views of a unit cell of the pulser array are shown. The unit cell has dimensions of $2b' \times 2a'$. In the ideal case of a plane wave incident on the interface (figure 4.1), there is but one value of Brewster angle ψ_B as already discussed. In the present realistic case of figure 4.2, the waves emanating at the switch gap are spherical and not planar. For an incident wave directed at an angle α with respect to the x axis, the Brewster angle for the conductor(s) is ψ_B. The angle α of the wave direction is measured from the -x axis, as viewed from above. The height $h(\alpha)$ of the conductor required to be placed between the switch gap and the interface, (side view of figure 4.2), is given by

$$\begin{aligned}
h(\alpha) &= \tan(\psi_B) \, \frac{b' - |x|}{\cos(\alpha)} \\
&= \tan(\psi_B') \, [b' - |x|]
\end{aligned} \tag{4.11}$$

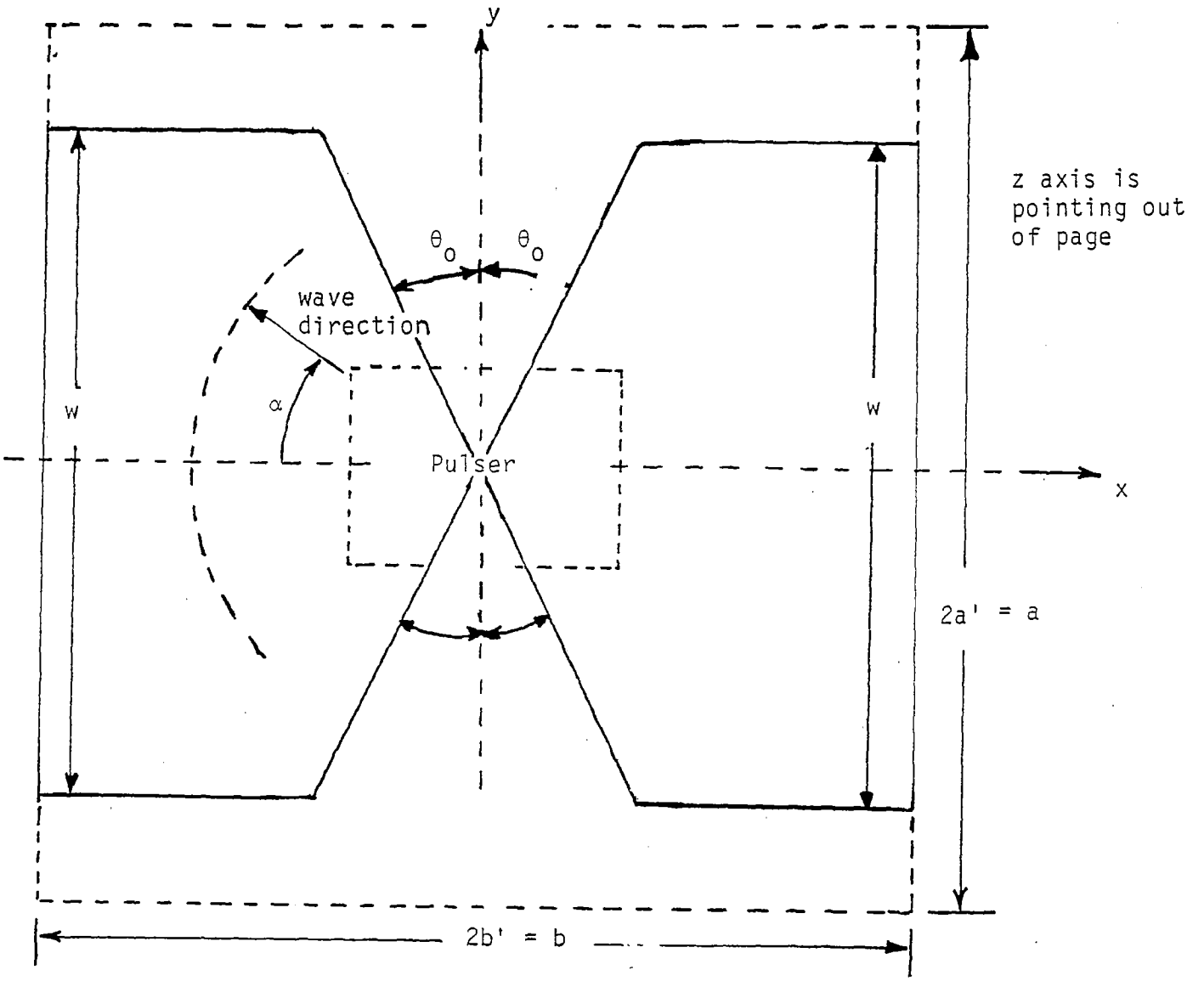

(a) Top View

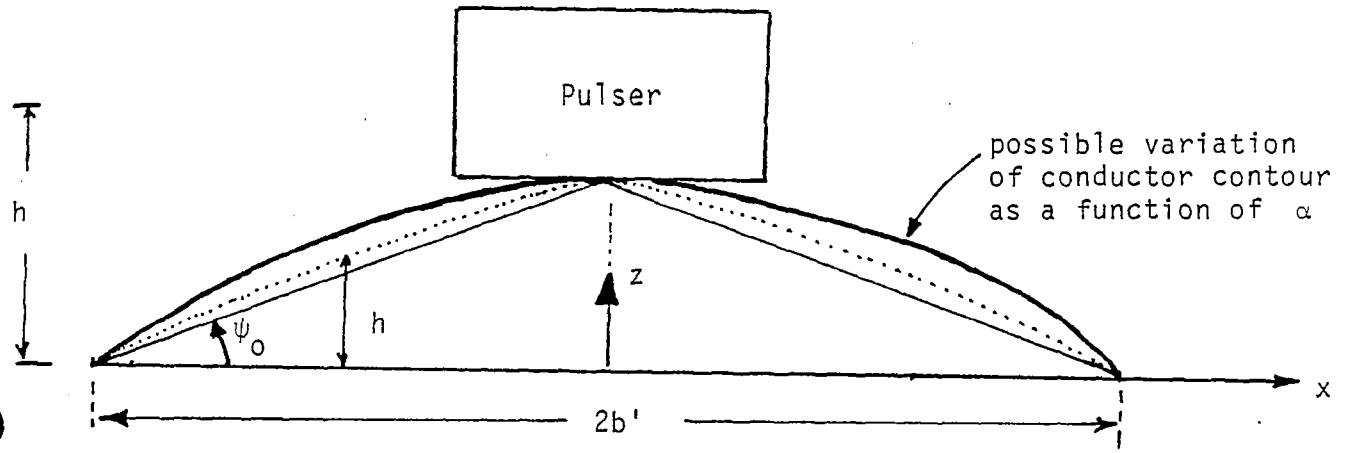

(b) Side View

Figure 4.2. Possible geometry of a unit-cell illustrating the variation in Brewster angle.

so that ψ_B' is an "effective" Brewster angle projected on the xz plane with

$$\tan(\psi_B') = \tan(\psi_B)/\cos(\alpha) \qquad (4.12)$$

It is observed that the above expression indicates a variation in the Brewster angle and may be interpreted as a larger height h as one moves away from the xz plane or decreasing α. One may conclude then that a certain optimization of the shaping of the conductor between the switch gap and the interface is essential, in order that the high-frequency Brewster angle concept be applicable. Such an optimization is perhaps best done experimentally.

Next, we turn our attention to the impedance that the pulser array drives for its unit cell.

B. Impedance of Unit Cell

A unit cell of the pulser array, schematically shown in figure 4.2(a) has the dimensions of $2a' \times 2b'$ in the $z = +h$ plane. If we consider times sufficiently greater than the transit times $\left[\sqrt{a'^2 + b'^2}\,/c\right]$ from the switch gap to the farthest point in the unit cell (a corner) as projected on the xy plane, the electric field is approximately parallel to the planes $y = \pm a'$ and $x = \pm b'$ may be considered as equipotentials. Under such an approximation, the impedance driven by a unit cell of the pulser array is given by

$$\tilde{Z}_{cell}(s) \simeq \sqrt{\frac{s\mu_o}{\sigma + s\varepsilon_r\varepsilon_o}}\, f_g$$

$$= \frac{Z_o}{\sqrt{\varepsilon_r}}\, f_g \left[1 + \frac{\sigma}{s\varepsilon_o\varepsilon_r}\right]^{-\frac{1}{2}} \qquad (4.13)$$

which at high frequencies, reduces to

$$\tilde{Z}_{cell}(s) \simeq \frac{Z_o f_g}{\sqrt{\varepsilon_r}} \qquad (4.14)$$

where the geometric factor f_g is

$$f_g = b'/a' \qquad (4.15)$$

In writing down the unit cell impedance above, the electromagnetic energy radiated above the unit cell $(z > h)$ has been neglected. Such an upward radiated field in general offer an additional load to the pulser in parallel with the ground load.

One may consider some illustrative cases as follows

example i) $\varepsilon_r = 10$ and $(b'/a') = 1$ (square cell)

$$\Rightarrow \tilde{Z}_{cell} \quad \text{(at high frequencies)} \simeq 119\ \Omega \tag{4.16}$$

example ii) $\varepsilon_r = 10$ and $(b'/a') = 0.5$ (rectangular cell)

$$\Rightarrow \tilde{Z}_{cell} \quad \text{(at high frequencies)} \simeq 60\ \Omega$$

In the above expressions, frequencies are high enough to satisfy the inequality

$$|s\varepsilon_o\varepsilon_r| \gg \sigma \tag{4.17}$$

and at high frequencies, the impedance driven by a unit cell is seen to be in the range of 60 Ω (rectangular cell with $b'/a' = 0.5$) to 120 Ω (square cell with $b'/a' = 1$). The effect of ground conductivity σ is to lower this impedance at lower frequencies.

Within the unit cell ($2a' \times 2b'$), the width of the conductor w may be crudely estimated as follows. In the yz plane, let the conductor of width w be at a height of h_o above the ground surface. For $w \gg h_o$, the transmission line formed by the conductor and the ground (assumed perfectly conducting) has an impedance

$$Z_o \frac{h_o}{w} \simeq \frac{\tilde{Z}_{cell}}{2} = Z_o \frac{b}{2w} \tan(\psi_B'') \tag{4.18}$$

where ψ_B'' is some average of ψ_B and ψ_B' discussed earlier. The above estimate is quite approximate and a more accurate estimation would consider the fringe fields around the edges and above the conductor. Note, however, that these fringe fields are in undesirable directions for matching into the ground within the unit cell. The inclusion of fringe fields leads to

$$\frac{\tilde{Z}_{cell}}{2} \simeq Z_o \frac{f_g'}{2} \tag{4.19}$$

with f_g' given as a function of $(2h_o/w)$ (see for example [11]). Using the simpler of the two approximations above, we have from (4.18),

$$\begin{aligned} \frac{w}{b} = \frac{w}{2b'} &= \frac{Z_o}{\tilde{Z}_{cell}} \tan(\psi_B'') \\ &\simeq \frac{Z_o}{\tilde{Z}_{cell}} \frac{1}{\sqrt{\varepsilon_r}} \end{aligned} \tag{4.20}$$

Substituting for $\tilde{Z}_{cell}$ from (4.14) and using (4.15), we have

$$\frac{w}{b} = \frac{w}{2b'} \simeq \frac{1}{f_g} = \frac{a'}{b'} = \frac{a}{b} \quad \text{or} \quad \frac{w}{a} \simeq 1 \tag{4.21}$$

For the two examples considered, we then have

i) rectangular cell $b'/a' = 1/2$

$$\frac{w}{2b'} \simeq 2 \quad \text{and} \quad \frac{w}{a} \simeq 1 \tag{4.22}$$

ii) square cell $b'/a' = 1$

$$\frac{w}{2b'} \simeq 1 \quad \text{and} \quad \frac{w}{a} \simeq 1$$

The above estimates of conductor width w are somewhat exagerated because of the fringe fields. However, it does point out that the optimal width w is close to almost the full value of the cell width a.

In what follows, we turn our attention to the impedance of the transition between a unit cell of the pulser array and the interface.

C. Impedance of Transition (conical model)

A possible geometry of the unit cell was illustrated in figure 4.2. In the gap region, where the high voltage source is applied, the conductors are narrow and receive current from a relatively small region. We may estimate the half angle of divergence θ_o of the gap using the results in [12]. This angle θ_o is small and also the conductors forming the gap region are assumed to be in a common plane $z = +h$. Equating the pulse impedance Z_g of the conical gap region [12] to the unit cell impedance $\tilde{Z}_{cell}$ derived earlier,

$$Z_g \simeq \frac{Z_o \pi}{4 \ell n \left[2 \cot\left(\frac{\theta_o}{2}\right)\right]} \simeq \tilde{Z}_{cell} \tag{4.23}$$

or

$$\ell n \left[2 \cot\left(\frac{\theta_o}{2}\right)\right] \simeq \frac{\pi}{4} \frac{Z_o}{\tilde{Z}_{cell}}$$

$$\simeq \frac{\pi}{4} \frac{\sqrt{\varepsilon_r}}{f_g} \simeq \frac{\pi}{4} \sqrt{\varepsilon_r} \frac{a'}{b'} \qquad (4.24)$$

or

$$\cot\left(\frac{\theta_o}{2}\right) \simeq \frac{1}{2} e^{\left[\frac{\pi}{4}\sqrt{\varepsilon_r} \frac{a'}{b'}\right]} \qquad (4.25)$$

or

$$\tan\left(\frac{\theta_o}{2}\right) \simeq 2 e^{-\left[\frac{\pi}{4}\sqrt{\varepsilon_r} \frac{a'}{b'}\right]} \qquad (4.26)$$

For the two examples considered earlier, we get

$$\text{example i)} \quad \frac{b'}{a'} = 1 , \ \varepsilon_r = 10 \Rightarrow \theta_o \simeq 19°$$

$$\text{example ii)} \quad \frac{b'}{a'} = 1/2 , \ \varepsilon_r = 10 \Rightarrow \theta_o \simeq 1.6° \qquad (4.27)$$

Employing the conical model of figure 4.2, it is seen that the half angle θ_o is too small and impractical from a high-voltage point of view. For this reason, we consider a modification in the pulser region as indicated in figure 4.3. The pulser can now be modelled as a gap between two metallic plates.

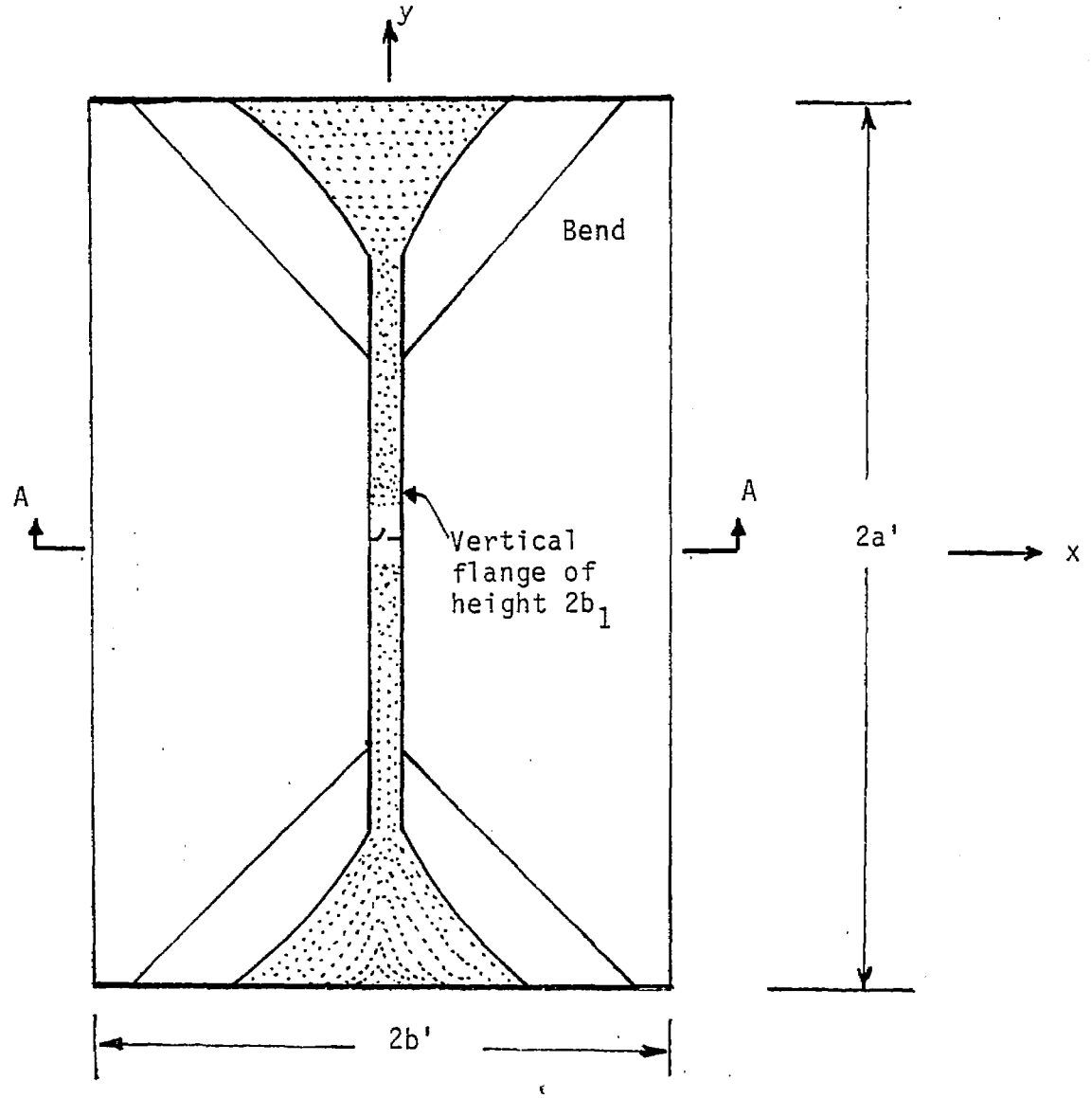

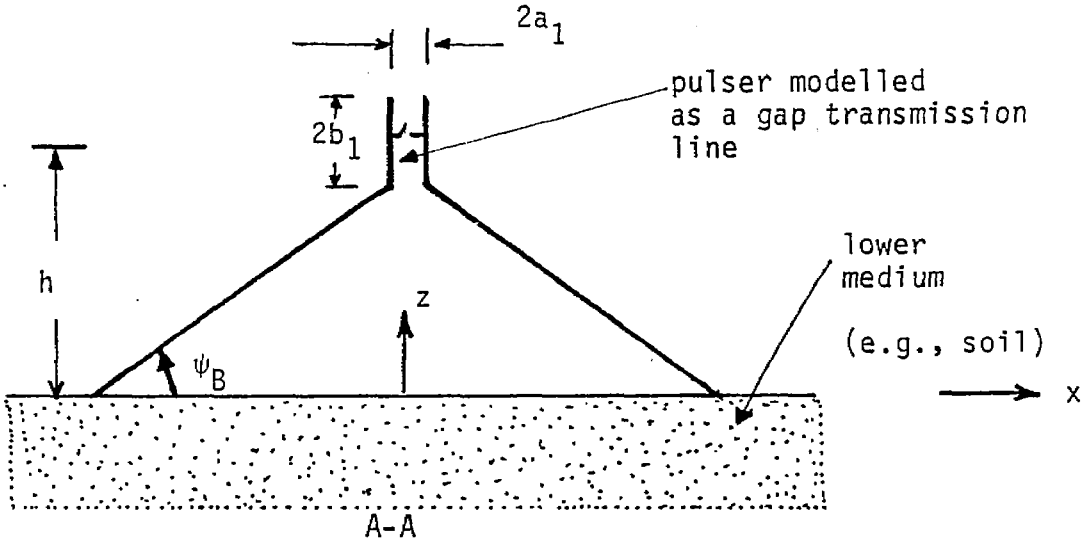

Figure 4.3. Unit cell geometry showing the pulser as a gap transmission line.

D. Impedance of Transition (Transmission Line Model)

If the unit cell dimensions are such that a' > b' (see figure 4.3), parallel plate metallic flanges may be introduced as a correction to the unit cell geometry. This parallel plate section can then be modelled as a transmission line and the source is symbolically represented as a switch across the plates. Make the effective impedance of the transmision line Z_{trans},

$$Z_{trans} = 2 Z_{cell} \tag{4.28}$$

to account for the two waves propagating on the transmission line away from the switch in the + and - y directions. Furthermore, corrections to the plates, at the ends may also be introduced to minimize the reflections. The height h as well as the flange separation $2 a_1$ and width $2b_1$ can be experimentally varied while monitoring the impedance matching via time doman reflectometry. Shaping or introduction of suitable bending in the butterfly like structure is also easily accomplished and is consistent with the earlier concept of the high-frequency Brewster angle required in eliminating or at least minimizing reflections at the interface.

In concluding this section, it is noted that some basic electromagnetic considerations involved in getting from the switch to the interface in a unit cell of the pulser array have been discussed above. However, in the practical implementation of these concepts, scale model experiments designed to optimize the conductor surfaces on one cell to start with, would be beneficial.

V. Summary

In this note we have addressed a general electromagnetic problem of coupling fields into the ground. The technique consists of a two-dimensional distribution of pulsers on a 'surface' parallel to and near the interface. The pulser array comprises of a unit cell repeating itself in the two directions. Electromagnetic considerations such as; the impedance driven by a unit cell, possible unit cell geometries in terms of matching the pulse impedance in the switch gap region to the cell impedance, exploiting the concept of high-frequency Brewster angle in order to minimize reflections off the interface, are discussed in this note. It is also observed that in the practical implementation of these ideas, carefully designed experimental optimization procedures are useful, especially in the context of shaping the conductor surfaces between the switch gap and the ground surface.

The usefulness of this technique lies in any application requiring the production and propagation of electromagnetic fields into a conducting (lossy) dielectric medium. Example applications include a) simulating natural lightning induced fields into ground, to study its coupling to buried systems, b) geological prospecting, c) detection of underground objects such as tunnels and d) simulation of EMP fields underground emanating an EMP near the interface.

References

1. C.E. Baum, "EMP Simulators for Various Types of Nuclear EMP Environments: An Interim Categorization", Sensor and Simulation Note 240, January 1978 and Joint Special Issue on the Nuclear Electromagnetic Pulse, IEEE Trans. on Antennas and Propagation, January 1978, pp. 35-53, February 1978, pp. 35-53.

2. C.E. Baum, "The Planar, Uniform Surface Transmission Line Driven from a Sheet Source", Sensor and Simulation Note 48, 10 August 1967.

3. C.E. Baum, "A Simplified Two-Dimensional Model for the Fields Above the Distributed-Source Surface Transmission Line", Sensor and Simulation Note 66, 20 December 1968.

4. C.E. Baum, "A Distributed Source Conducting-Medium Simulator for Near and Below the Ground Surface", Sensor and Simulation Note 87, 9 July 1969.

5. F.C. Yang, "A Distributed Source-Region EMP Simulator", Sensor and Simulation Note 266, July 1980.

6. J.A. Stratton, Electromagnetic Theory, McGraw-Hill, New York, 1941.

7. S. Ramo, J.R. Whinnery and T. Van Duzer, Fields and Waves in Communication Electronics, John Wiley and Sons, Second edition, 1984.

8. C.E. Baum, "The Brewster Angle Wave Matcher," Sensor and Simulation Note 37, 13 March 1967.

9. C.D. McGillem and G.R. Cooper, Continuous and Discrete Signal and System Analysis, Holt, Rinehart and Winston, Second edition, 1984.

10. J.H. Scott, "Electrical and Magnetic Properties of Rock and Soil", Theoretical Note 18, 26 May 1966.

Referneces (concluded)

11. C.E. Baum, D.V. Giri and R.D. Gonzalez, "Electromagnetic Field Distribution of the TEM Mode in a Symmetrical Two-Parallel-Plate Transmission Line", Sensor and Simulation Note 219, 1 April 1976.

12. C.E. Baum, "A Conical-Transmission-Line Gap for a Cylindrical Loop", Sensor and Simulation Note 42, 31 May 1967.